Journal of Nuclear Medicine, published on October 12, 2011 as doi:10.2967/jnumed.111.090266

Combined RNA Interference of Hexokinase II and ^{131}I-Sodium Iodide Symporter Gene Therapy for Anaplastic Thyroid Carcinoma

Jung Eun Kim, Byeong-Cheol Ahn, Mi-Hye Hwang, Yong Hyun Jeon, Shin Young Jeong, Sang-Woo Lee, and Jaetae Lee

Department of Nuclear Medicine, Kyungpook National University School of Medicine, Daegu, South Korea

The purpose of this study was to investigate the enhanced therapeutic effect of the combined use of shRNA (small hairpin RNA) therapy for the hexokinase II (HKII) gene and ^{131}I human sodium iodide symporter (hNIS) as a gene therapy for in vitro and in vivo treatment of anaplastic thyroid carcinoma cells (ARO) in an animal model. **Methods:** A recombinant lentivirus containing a plasmid with the hNIS gene driven by phosphoglycerate kinase promoter and green fluorescent protein (GFP) linked with an internal ribosome entry site sequence was produced. ARO cells were transfected with the virus and sorted by fluorescent activated cell sorting using GFP (ARO-NG). The messenger RNA expression of hNIS and GFP were evaluated with reverse-transcriptase polymerase chain reaction, and the function of hNIS was verified by ^{125}I uptake. The lentiviral vector expressing shRNA against HKII (Lenti-HKII shRNA) was constructed and used to infect ARO-NG cells. The effect of Lenti-HKII shRNA was evaluated by reverse-transcriptase polymerase chain reaction, ^{18}F-FDG uptake, and HK activity. An in vitro clonogenic assay was performed after Lenti-HKII shRNA therapy, ^{131}I therapy, and a combined therapy. The therapies were also applied in vivo to an animal model with an ARO-NG xenograft, and the effects were assessed with caliper measurements and ^{18}F-FDG PET. **Results:** ARO-NG cells showed an ^{125}I uptake 76-fold higher than the parent ARO cells. Compared with the uninfected ARO-NG cells, ARO-NG cells infected with Lenti-HKII shRNA had lower HKII messenger RNA expression, lower ^{18}F-FDG uptake, and HK activity. The proliferation of ARO-NG cells was inhibited by ^{131}I and Lenti-HKII shRNA therapies and further inhibited by the combined ^{131}I and Lenti-HKII shRNA therapy. Both the Lenti-HKII shRNA therapy and the ^{131}I therapy inhibited in vivo tumor growth in the tumor xenograft model. The combined Lenti-HKII shRNA and ^{131}I therapy resulted in a further decrease of tumor growth. **Conclusion:** Our results suggest that the combined HKII shRNA and ^{131}I therapy has a stronger antitumor effect than either the ^{131}I therapy or the HKII shRNA alone. Therefore, this combined therapy could be used as a powerful strategy for treating anaplastic thyroid carcinoma.

Key Words: combination therapy; gene therapy; hexokinase II shRNA; human sodium iodide symporter; radioiodine therapy

J Nucl Med 2011; 52:1–8
DOI: 10.2967/jnumed.111.090266

Received Mar. 13, 2011; revision accepted Jul. 5, 2011.
For correspondence or reprints contact: Byeong-Cheol Ahn, Department of Nuclear Medicine, Kyungpook National University School of Medicine, 50 Samduk-dong 2-ga, Chung Gu Daegu, South Korea, 700-721.
E-mail: abc2000@mail.knu.ac.kr
COPYRIGHT © 2011 by the Society of Nuclear Medicine, Inc.

Anaplastic thyroid cancer (ATC) is the most aggressive form of thyroid malignancy, with a mean survival time of just a few months, although this can vary according to various prognostic factors (*1,2*). Several types of treatment methods such as surgery, radiotherapy, chemotherapy, or a combination of these modalities have been applied for treating this cancer. However, there is currently no standardized successful treatment strategy (*3*). Therefore, development of new effective therapeutic strategies is urgently needed.

Many cells produce energy by glycolysis followed by lactic acid fermentation in the cytosol rather than by mitochondrial oxidation of pyruvate. The metabolic alteration of cancer cells is known as the Warburg effect (*4,5*); these cells have a high metabolic rate and accumulate glucose at a higher rate than the normal surrounding tissues (*6*). Hexokinase (HK) catalyzes the first step of cellular glycolysis and plays important roles in essential homeostatic processes such as glucose metabolism and cell apoptosis (*7*). Among the 4 HK isoforms (HKI–HKIV), HKII is known to be highly expressed in many tumor cells (*8*).

Double-stranded RNA interference (RNAi) is a simple and rapid method to repress the expression of a targeted gene (*9,10*). RNAi using small interfering RNA (siRNA) specific for HKII has been implemented to inhibit HKII gene expression and precludes proliferation of cancer cells (*11,12*). However, siRNA is known to be degraded in cells within a few days. Contrary to siRNA, small hairpin RNA (shRNA) is integrated into chromosomal DNA and is constantly expressed to achieve prolonged gene silencing (*13*). The major advantage of the lentiviral shRNA system is that the shRNA can be delivered into both dividing and nondividing cells to achieve stable long-term effects on target gene silencing; therefore, it can be used for in vivo applications (*14*). Recently, many studies reported the use of retroviral- and lentiviral-based vector systems for the expression of shRNAs for cancer therapy (*15,16*). However, to the best of our knowledge, there has been no therapeutic trial of a lentiviral shRNA system targeting HK in a tumor xenograft animal model.

The sodium iodide symporter (NIS) is an intrinsic membrane protein with 13 transmembrane domains. It

inm090266-pm ■ 10/12/11
Copyright 2011 by Society of Nuclear Medicine.

simultaneously takes up 2 sodium and 1 iodide molecules into the cytosol from extracellular fluid in a process driven by low internal sodium concentration in the thyroid epithelial cells, via facilitated diffusion, caused by the sodium–potassium adenosine triphosphatase pump (*17*). Because of its efficient iodine uptake function, NIS has been used for imaging normal thyroid tissue or differentiated thyroid carcinoma with ^{123}I or ^{99m}Tc, as well as treating differentiated thyroid carcinomas and their metastases using ^{131}I (*18,19*). Radioiodine therapy after NIS gene transfer has been suggested as a novel treatment modality for several cancers that lack NIS expression (*20*). However, this type of therapy has limited effects and can produce serious adverse side effects related to radioiodine dose (*21*). Reducing the radioiodine dose for NIS gene therapy can mitigate the adverse side effects but might lead to limited therapeutic effectiveness.

Although a single-modality gene therapy using HKII RNAi or the NIS gene can be applied to treat cancer, these therapeutic approaches have their own side effects and limitations. Therapeutic effect is usually correlated with a dose of the treatments, and severity of the side effects is almost always tightly associated with the dose. A combined therapeutic approach using both strategies would be more efficient for improving therapeutic outcome and can diminish adverse effects better than a single therapeutic approach by reducing doses. In this study, we investigated the in vitro and in vivo effects of a combined therapy with lentiviral shRNA targeting HKII and human NIS (hNIS) gene expression with radioiodine treatment on ATC in an animal model.

MATERIALS AND METHODS

Establishment of ARO Cells Expressing hNIS Gene (ARO-NG)

The cells were grown in RPMI medium (Gibco) containing 10% fetal bovine serum (Hyclone) and 1% penicillin–streptomycin (Gibco). The cells were transfected with a recombinant lentivirus with a plasmid containing both hNIS and green fluorescent protein (GFP) driven by a phosphoglycerine kinase (PGK) promoter (pLenti/PGK-hNIS-internal ribosome entry site GFP). The pLenti/PGK-hNIS-IRES-GFP vector was kindly provided by Dr. June-Key Chung (Seoul National University). The GFP fluorescence of the cells was analyzed with fluorescent microscopy (Nikon Eclipse Ti-S; Nikon Inc.). The cells expressing hNIS and GFP were sorted with flow cytometry (FACSorter; BD Biosciences).

Production of Lentiviral Particles Containing HKII shRNA

We designed the HKII-targeting sequence (5′-GGATGTGTGTGAACATGGAAT-3′; GenBank accession no. NM_000189.4). These micro-RNA gene double strands were ligated with Block-iT Pol II miR RNAi Expression Vector (Invitrogen) containing EmGFP gene. Inserts targeting the HKII messenger RNA (mRNA) were cloned into an expression vector plasmid to construct recombinant plasmid pcDNA6.2-HKII-miR. Recombinant plasmid pcDNA6.2-HKII-miR was cloned into Block-iT Lentiviral Pol II miR RNAi Expression System (Invitrogen). All of the cloned constructs were verified by sequencing. Recombinant lentivirus was cotransfecting 293FT cells with the lentivirus expression plasmid and packaging plasmids using the calcium phosphate method. Lentivirus was harvested 48 h after transfection and filtered, and infectious titers were determined by fluorescence activated cell–sorting analysis of EmGFP-positive HT1080 cells and expressed as transduction units per milliliter (TU/mL).

Reverse-Transcriptase Polymerase Chain Reaction Analysis for hNIS and GFP Genes

Total RNA was extracted from ARO and ARO-NG cells using Trizol reagent (Invitrogen) according to the manufacturer's instruction. Reverse-transcriptase polymerase chain reaction was performed using a complementary DNA synthesis kit (Fermentas). The following primers were used: hNIS, forward: 5′-CGCTGGCCCAGAACCATC-3′, reverse: 5′-AAAATCTAGAGTCAGAGGTTTGTCTCCTGCT-3′; GFP, forward: 5′-CAGCCACAACGTTATCA-3′, reverse: 5′-GTGTTCTGCTGGTAGTGGTC-3′; and glyceraldehyde-3-phosphate dehydrogenase (GAPDH), forward: 5′-TGCCACCCAGAAGACTGTG-3′, reverse: 5′-ATGTGGGCCATGAGGTCCAC-3′.

Confocal Microscopy for hNIS

For confocal microscopy analysis, cells were seeded at 2×10^4 cells in a Lab-Tek cover glass (Nagel Nunc Int.). Subsequently, the cells were incubated with a primary antibody against hNIS (mouse anti-hNIS, 1:200 dilution; Molecular Probes, Inc.) at room temperature for 1 h. The cells were then incubated with a secondary antibody (Alexa 568 goat antimouse, 1:150 dilution; Milipore) at room temperature for 40 min, and then 4′,6-diamidino-2-phenylindole staining.

^{125}I Uptake Study

The cells were plated in a 24-well plate at different cell numbers ranging from 0.125×10^6 to 1×10^6 cells per well. ^{125}I uptake was measured using the method by Lee et al. (*20*). After 30 min of incubation, the cells were lysed with 2% sodium dodecyl sulfate. The radioactivity was measured using a γ-counter (Cobra II; Canberra Packard, Packard Bioscienece). The radioactivity of the cells was normalized using total protein concentrations determined by a BCA kit (Pierce). The iodine uptake is expressed as pmol/mg of protein.

In Vitro ^{18}F-FDG Uptake Assay

The 0.5×10^5 cells were seeded in each well of a 24-well plate and infected with Lenti-HKII shRNA (4×10^7 TU/mL) in the presence of hexadimethrine bromide (Polybrene; Abbott Laboratories Corp.) (10 μg/mL) for 24 h. ^{18}F-FDG uptake was determined at 72 h after transfection by incubating the cells with Hank balanced salt solution containing 0.5% bovine serum albumin and 74 kBq of ^{18}F-FDG per milliliter for 30 min at 37°C. The collection of cell lysate and the measurement of radioactivity and the protein contents of the supernatants were also performed as described for the ^{125}I uptake study.

HK Activities in ARO-NG Cells Treated with Lenti-HKII shRNA

Total HK activity was measured using the method of Vinuela et al. (*22*), with modifications. Briefly, 3×10^5 cells plated in 6-well plates were treated with Lenti-HKII shRNA or Lenti-scramble shRNA. After 72 h, the cells were harvested into solution I (0.05 M triethanol amine, 0.3 M $MgCl_2$, and HCl), and the lysates were

jnm090266-pm ■ 10/12/11

homogenized. The homogenates were centrifuged, and the supernatants were assayed. The protein contents of the supernatants were also measured.

In Vitro Clonogenic Assay

ARO and ARO-NG cells were plated in T-75 culture flasks (5×10^6 cells per flask) followed by the addition of 14.8 MBq of ^{131}I in Hank's balanced salt solution containing 0.5% bovine serum albumin. After 7 h of exposure, the 1,000 cells were plated into each well of 6-well culture plates. On day 7, the cells were stained with a crystal violet solution. Colonies having more than 50 cells were counted, and the mean and SD values were determined. The results are expressed as the percentage of the number of colonies relative to that of the control. For the in vitro combination therapy, ARO and ARO-NG cells (5×10^6 cells per flask) were incubated in bHBSS containing 14.8 MBq of ^{131}I for 7 h and then seeded in 6-well plates at 1,000 cells per well. Lenti-HKII shRNA (4×10^7 TU/mL) was used to transfect each well 4 d after the ^{131}I treatment. On day 3 after the lentiviral transfection, the number of colonies containing more than 50 cells was determined.

Small-Animal PET with ^{18}F-FDG

All animal experiment protocols were approved by the Committee for the Handling and Use of Animals of Kyungpook National University. An in vivo imaging study was performed on 25 mice using the following procedures. ARO and ARO-NG cells (5×10^6/100 μL) were subcutaneously injected in the right thigh of BALB/c nude mice ($n = 5$; Japan SLC Inc.); at 14 d after inoculation, 3.7 MBq of ^{18}F-FDG were intravenously administered to the mice, and then imaging was performed using a micro-PET R4 (Concorde Microsystems Inc.) with an approximate resolution of 2 mm in each axial direction.

Combined Therapy in In Vivo Animal Tumor Model

The protocol for the in vivo combined therapy is shown in [**Fig. 1**] Figure 1. The mice were divided into 5 groups containing 5 mice in each group: the control (intratumoral injection of phosphate-buffered saline [PBS]), Lenti-scramble shRNA (4×10^7 TU/mL) therapy, Lenti-HKII shRNA (4×10^7 TU/mL) therapy, ^{131}I therapy (55 MBq), and combined Lenti-HKII shRNA and ^{131}I therapy group (Lenti-HKII shRNA: 4×10^7 TU/mL, ^{131}I: 55 MBq). Mice were treated with the Lenti-scramble shRNA or Lenti-HKII shRNA on days 1 and 4. PBS and ^{131}I were intraperitoneally injected at the same time as the initial Lenti-HKII shRNA treatment. Tumor volume was measured with calipers every week for 21 d after therapy. For small-animal PET, 30 min after a tail vein injection of 3.7 MBq of ^{18}F-FDG, images were acquired for 20 min. The images were reconstructed with a 2-dimensional ordered-subsets expectation maximum algorithm. Corrections were not required for attenuation or scattering. Activity was quantified by viewing the region of interest in the tumors and averaging the activity concentrations over the contained voxels. ^{18}F-FDG uptake was expressed as the percentage injected dose per gram of tumor volume (%ID/g). Tumor-bearing mice were maintained under isoflurane (Forane; ChoongWae Co.) anesthesia during the injection, accumulation, and scanning periods. Mice received T4 supplementation (5 mg/L) in their drinking water for 2 wk before ^{131}I administration. The therapy was started when the tumor size reached 5 mm in diameter.

Statistical Analysis

All data are expressed as the mean ± SD. The statistically significant differences were assessed by Mann–Whitney U test and Kruskal–Wallis 1-way ANOVA. P values of less than 0.05 were considered to be statistically significant.

RESULTS

Establishing ARO-NG Cells with ARO Cells and Verification of Gene Expression

ARO cells were transfected with lentivirus containing hNIS, GFP genes were analyzed with flow cytometry, and 14% of the cell population with the highest GFP was sorted out by cytometry. These cells were cultured for several days, and then the GFP was analyzed with florescent microscopy. Almost all (97%) of the cells, named ARO-NG, were GFP-positive and used for this experiment (Supplemental Fig. 1; supplemental materials are available online only at http://jnm.snmjournals.org). Reverse-transcriptase polymerase chain reaction showed that hNIS and GFP mRNA were expressed in ARO-NG cells but not in the parent ARO cells (Supplemental Fig. 2). GFP expression (upper right, green) was

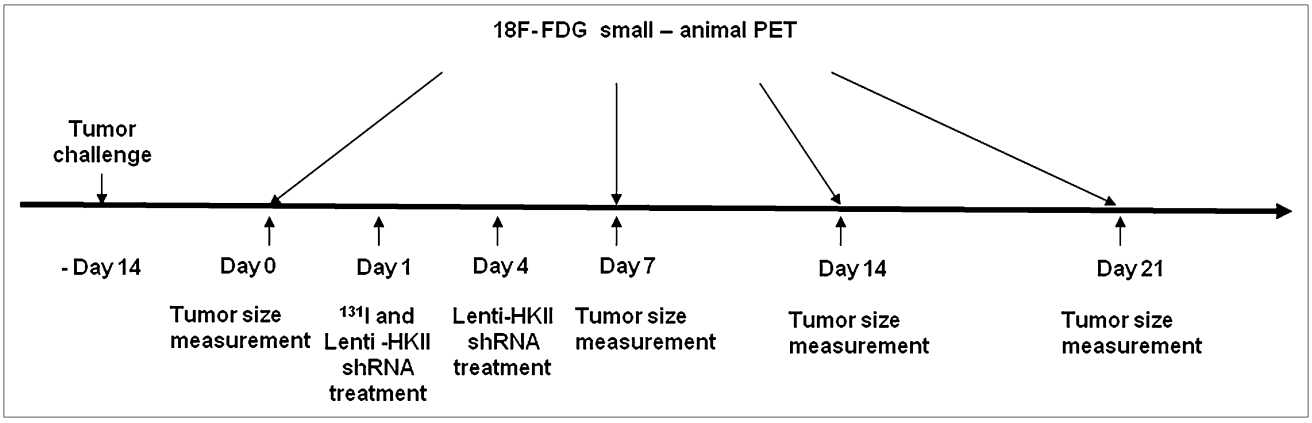

FIGURE 1. In vivo experimental schedule of combined Lenti-HKII shRNA and ^{131}I therapy. BALB/c nude mice were challenged with 5×10^6 ARO-NG cells by subcutaneous injection into right hind limbs and then were treated with PBS, Lenti-scramble shRNA, or Lenti-HKII shRNA by intratumoral injection on days 1 and 4. ^{131}I was intraperitoneally injected during initial administration of Lenti-HKII shRNA therapy. Tumor size was measured with calipers every week, and tumor volume was calculated using formula $m1^2 \times m2 \times 0.5236$ (where $m1$ represents length of short tumor axis and $m2$ represents that of long tumor axis) until day 21 after therapy.

jnm090266-pm ■ 10/12/11

observed throughout cells, and hNIS expression was detected mainly on the cell membrane by immunostaining with anti-hNIS antibody (lower left, red). The combined image of the immunostaining and 4′,6-diamidino-2-phenylindole staining (lower right) showed the cell membrane localization of hNIS [Fig. 2] (Fig. 2).

Assessment of Functional Activity of hNIS In Vitro

The in vitro radioiodine uptake was assessed in ARO and ARO-NG cells. ARO-NG cells showed more than a 76-fold increase in iodine uptake of 1×10^6 cells than the ARO cells. In the radioiodine uptake assay performed to assess functional hNIS gene expression, iodine uptake of the ARO-NG cells was increased in a cell number–dependent fashion, but this was not observed in ARO cells (Supplemental Fig. 3).

Change of HKII mRNA Expression, ^{18}F-FDG Uptake, and Total HK Activities by Lenti-HKII shRNA

Lenti-HKII shRNA treatment resulted in markedly decreased expression of HKII mRNA in ARO-NG cells at 72 h, compared with the control cells or cells transfected with Lenti-scramble shRNA (Supplemental Fig. 4A). In addition, the proliferation rate of ARO-NG cells decreased with Lenti-HKII shRNA treatment (Supplemental Fig. 4B). In ARO-NG cells, Lenti-HKII shRNA treatment resulted in a 40% ± 7.9% decrease of ^{18}F-FDG uptake, compared with [Fig. 3] that of untreated ARO-NG cells (Fig. 3). There was not a significant difference in ^{18}F-FDG uptake between untreated and Lenti-scramble shRNA-treated ARO-NG cells. The level of HK activity of ARO-NG cells treated with Lenti-HKII shRNA decreased to 75.9% ± 7.7%, compared with [Table 1] that of the control cells (Table 1).

In Vitro Cell Survival Study with Clonogenic Assay

The colony-forming ability of ARO-NG cells was decreased to 58% ± 8.1% by 14.8 MBq of ^{131}I and 64.5% ± 8.4% by Lenti-shRNA HKII treatment (4×10^7 TU/mL). This ability was further decreased to 29% ± 8.8% by a combined ^{131}I and Lenti-HKII shRNA treatment (Fig. 4). [Fig. 4]

In Vivo Effects of Lenti-HKII shRNA, ^{131}I, and Combined Therapy in Animal Model

Tumors regressed or tumor growth was significantly inhibited on days 7–21 after treatment in mice treated with Lenti-HKII shRNA, ^{131}I, or the combined therapy, compared with mice treated with PBS or Lenti-scramble shRNA (Fig. 5A). Differences in tumor volume between [Fig. 5] the treatment, control, and Lenti-scramble shRNA therapy groups were noticeable starting on day 7 after the therapy began. Tumor volumes (Lenti-HKII shRNA therapy, 116.3% ± 38.4%; ^{131}I therapy, 70.7% ± 22.4%; combined therapy, 44.2% ± 16.0%, compared with the tumor volume on day 0) of the therapy groups were significantly smaller than those of control and Lenti-scramble shRNA therapy groups (464.1% ± 139.6% and 422.6% ± 178.9%, respectively, compared with the tumor volume on day 0). As shown in Figure 5B, mice treated with the combined therapy had a smaller tumor volume on day 14 (17.8% ± 8.1%, compared with the day 0 tumor volume) and on day 21 (0.1% ± 0.04%, compared with the day 0 tumor volume) than those of mice treated with the Lenti-HKII shRNA and ^{131}I single therapies (139.4% ± 61.4% and 59.0% ± 22.0%, respectively, on day 14, compared with the day 0 tumor volume, and 130.8% ± 86.5% and 31.0% ± 4.4%,

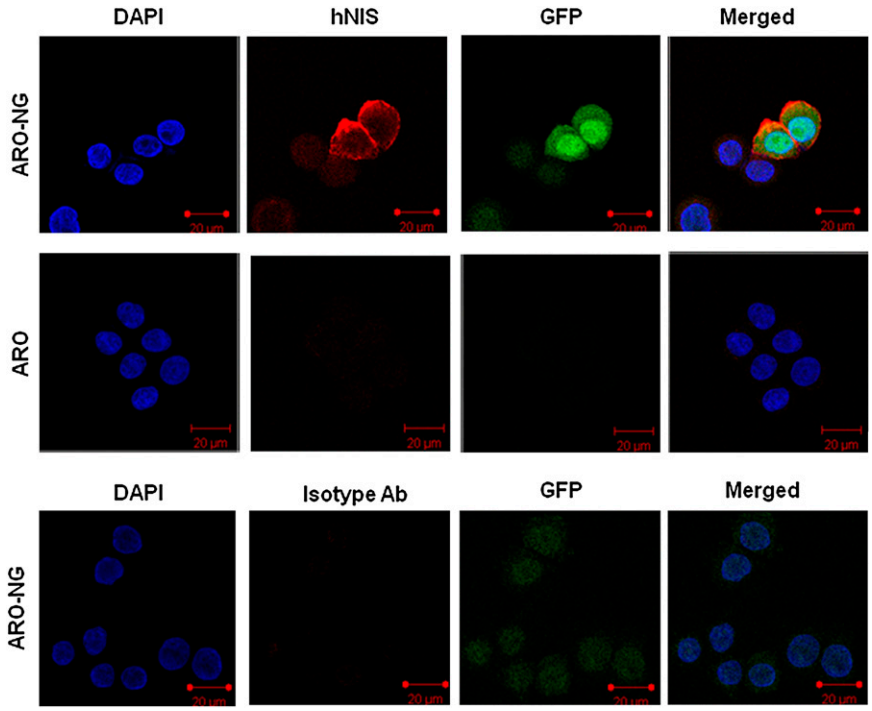

FIGURE 2. Immunohistochemistry with anti-hNIS antibody in ARO-NG cells using confocal microscopy. Cell nuclei were visualized with 4′,6-diamidino-2-phenylindole staining (blue). GFP expression (green) was observed throughout cells, and hNIS expression was mainly detected on cell membrane (red). Merged image showed true location of hNIS in cells, which was expected to be on cell membrane. Parent ARO cells did not show GFP or hNIS staining. DPAI = 4′,6-diamidino-2-phenylindole.

jnm090266-pm ■ 10/12/11

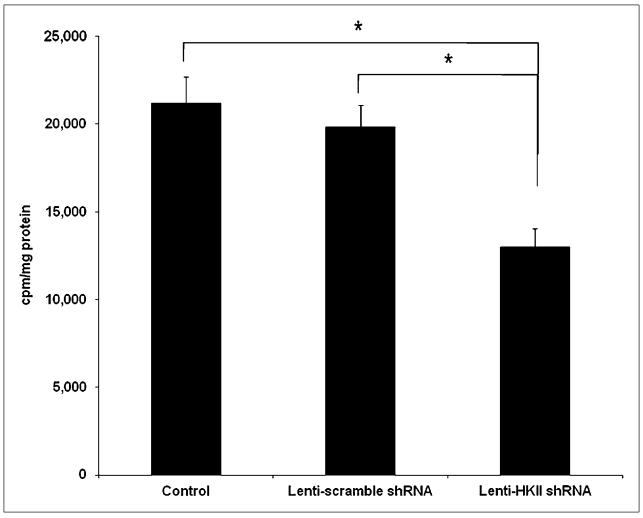

FIGURE 3. In vitro ^{18}F-FDG uptake measured 72 h after Lenti-HKII shRNA or Lenti-scramble shRNA transfection in ARO-NG cells. Cells transfected with Lenti-HKII shRNA showed lower ^{18}F-FDG uptake than cells treated with PBS or Lenti-scramble shRNA. *Mean $P < 0.05$.

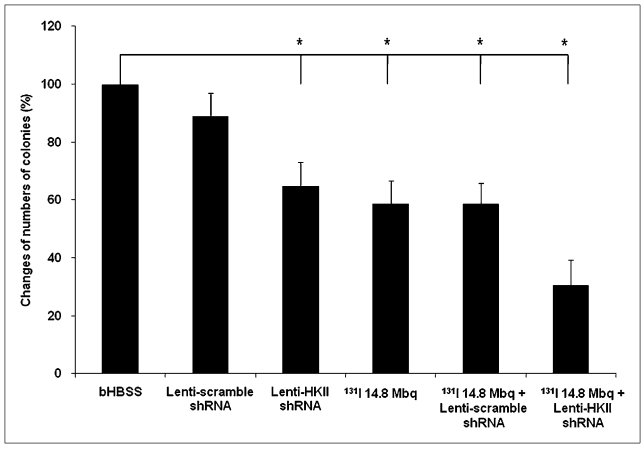

FIGURE 4. In vitro clonogenic assay for cell survival on day 3 after Lenti-HKII shRNA or on day 7 after ^{131}I therapy or combined Lenti-HKII shRNA and ^{131}I therapy. Clone-forming ability of ARO-NG cells was inhibited 58% ± 8.1% by ^{131}I or 64.5% ± 8.4% by Lenti-HKII shRNA therapy alone and further inhibited 29% ± 8.8% by combined ^{131}I and Lenti-HKII shRNA therapy. *Mean $P < 0.05$.

respectively, on day 21, compared with the day 0 tumor volume).

The response of tumors was clearly visible on the small-animal PET images of all mice (Fig. 6A). ^{18}F-FDG uptake of the tumor in the control and Lenti-scramble shRNA therapy groups (3.49 ± 0.13 %ID/g and 3.20 ± 0.15 %ID/g, respectively) on day 7 is shown in Figure 6B. Mice treated with either Lenti-HKII shRNA or ^{131}I or the combined therapy showed lower ^{18}F-FDG uptake (1.96 ± 0.10, 1.99 ± 0.09, and 2.02 ± 0.04 %ID/g, respectively) than those of the control and Lenti-scramble shRNA therapy groups and had a significant difference in ^{18}F-FDG uptake 7 d after starting the therapies. As shown in Figure 6B, reduction of ^{18}F-FDG uptake by the combination therapy was demonstrated after day 14 (2.42 ± 0.07 %ID/g, Lenti-HKII shRNA; 1.98 ± 0.10 %ID/g, ^{131}I; and 1.61 ± 0.09 %ID/g, combined therapy); the combined therapy produced the most effective response, compared with any other single therapy (3.01 ± 0.10 %ID/g, control, and 3.21 ± 0.11 %ID/g, Lenti-scramble shRNA therapy). Reduction of ^{18}F-FDG uptake by the combination therapy (Fig. 6B) was also demonstrated after day 21 (2.47 ± 0.15 %ID/g, Lenti-HKII shRNA; 2.01 ± 0.05 %ID/g, ^{131}I; and 1.62 ± 0.05 %ID/g, combined therapy) and produced the most effective therapeutic response, compared with any other single therapy (2.86 ± 0.18 %ID/g, control, and 3.10 ± 0.19 %ID/g, Lenti-scramble shRNA).

[**Fig. 6**]

TABLE 1
HK Activities in ARO-NG Cells

Treatment	HK activity ($n = 3$) (mU/mg of protein)
None (control)	14.24 ± 3.59
Lenti-scramble shRNA	13.46 ± 2.53
Lenti-HKII shRNA	4.52 ± 0.65*

*$P < 0.05$ compared with control.

DISCUSSION

RNAi allows specific reduction of disease-associated genes and is applicable for any gene with a complementary sequence; the silencing of critical cancer-associated target genes by siRNAs has resulted in significant antiproliferative or apoptotic effects (*23*). RNAi assays using chemically synthesized siRNAs are reliable for short-term studies of gene expression; however, they are costly and limit the number and scale of experiments that can benefit from this technique. To solve these issues, a shRNA system for the stable expression of siRNAs had been developed (*24*).

In the previous reports by Peng et al., a stable cell line expressing HKII shRNA was made and retarded tumor growth, but no tumor elimination was observed (*25*). This group demonstrated the effects of HKII silencing on tumor cell growth, but their system is artificial and not applicable to clinical situations. An in vivo HKII shRNA delivery system should be developed for clinical application. For this, a lentiviral shRNA delivery system can be an option because of its long-term effect and high gene transduction efficiency in both dividing and nondividing cells (*13*). In the current study, we successfully inhibited HKII gene expression, decreased glucose uptake, and decreased HK activity with lentiviral vector–mediated HKII shRNA delivery. We also found that treatment with the virus in vitro and in vivo significantly inhibited ARO cell proliferation. As expected, the virus prevented tumor growth but did not eradicate the tumor because of the viral cytostatic effect rather than cytotoxic effect. The limited therapeutic effect of the virus might be related to the fact that shRNA specific

jnm090266-pm ■ 10/12/11

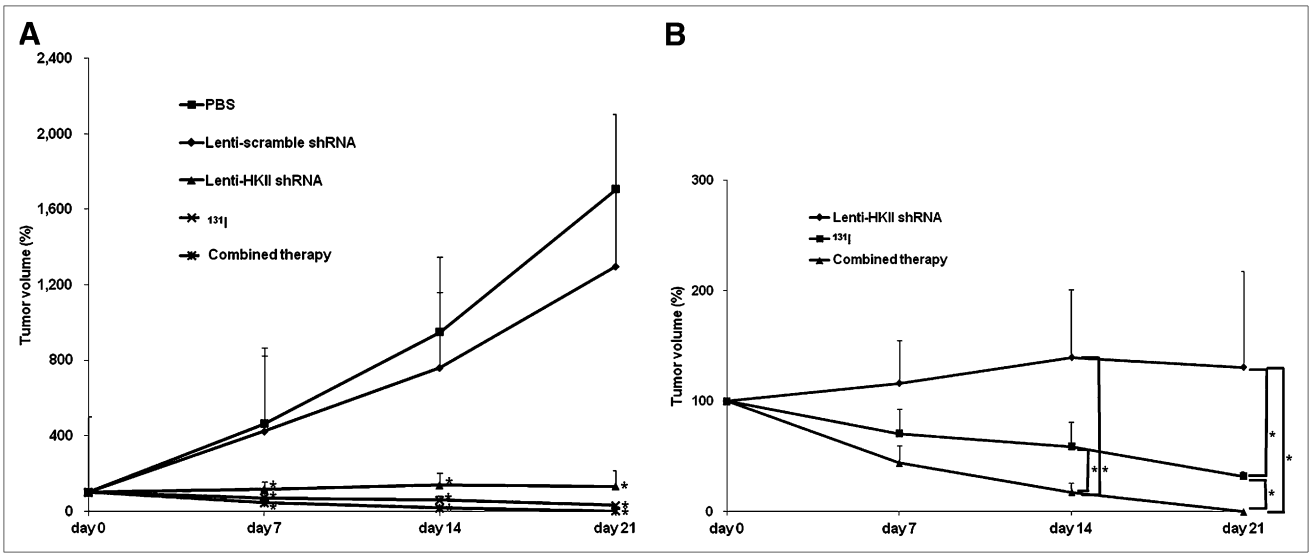

FIGURE 5. (A) In vivo effects of Lenti-HKII shRNA and ^{131}I therapy on ARO-NG tumor xenografts in animal model. Tumor volumes of all therapy groups were significantly smaller than those of control and Lenti-scramble shRNA therapy groups. *Mean $P < 0.05$. †Mean $P < 0.001$. (B) Tumor volumes of ^{131}I therapy group were significantly smaller than those of Lenti-HKII shRNA therapy group on day 21. Tumor volumes of combined therapy group were significantly decreased, compared with other individual therapy groups on days 14 and 21. *Mean $P < 0.05$.

for HKII cannot completely block glucose metabolism because of the presence of other HK isotypes and that various pathways that produce energy other than glucose metabolism are also available in cancer cells (*25*). Therefore, the use of other therapeutic modalities such as radioiodine and hNIS gene therapy in addition to Lenti-HKII shRNA therapy might be needed to cure cancer.

Differentiated thyroid carcinoma with hNIS expression responds to ^{131}I therapy; however, most ATCs respond poorly to this therapy because of their inability to accumulate iodine (*26*). Several investigators have suggested the use of radioiodine therapy after exogenous hNIS gene expression in anaplastic thyroid carcinoma or other nonthyroid cancers that lack hNIS expression (*19–21,27,28*). These results suggest that hNIS gene transfer may be used for cancer therapy by restoring or inducing radioiodine uptake in various cancer cells. However, radioiodine treatment with hNIS gene therapy has limited effects with therapeutic doses of radioiodine and can cause serious side effects if high doses are administered (*21,29*). Results of this study also showed that 55.5 MBq (1.5 mCi) of ^{131}I does not incur serious side effects but has limited therapeutic antitumor effects. Therefore, the additional use of other therapeutic strategies, such as chemotherapy or external radiotherapy, is necessary to treat cancer and achieve therapeutic goals without severe adverse effects related to the radioiodine therapy. ATC has been characterized and classified as distinct from differentiated thyroid carcinoma by a higher percentage of HKII in the mitochondrial fraction (*30*). In particular, mitochondrion-bound HKII is correlated with high glycolytic rates in tumors, and inactivation of this enzyme can retard tumor growth by inhibiting glucose metabolism, which is enhanced in most tumor cells (*31,32*). We hypothesized that hNIS gene therapy with a safe dose of radioiodine could be used to treat cancer but might have limited cytotoxic effects. Therefore, the additional use of another therapeutic modality that induces tumor growth inhibition, such as Lenti-HKII shRNA therapy, along with radioiodine and hNIS gene therapy might be required to treat cancer.

In this study, radioiodine with hNIS gene therapy or Lenti-HKII shRNA therapy alone or a combined therapy was administered to evaluate the potential enhanced therapeutic effects of the combined therapy, compared with the individual therapies alone on ATC in vitro and in vivo. We found that the combined therapy was more effective for treating the tumors than the Lenti-HKII shRNA or ^{131}I therapies alone. With the combined therapy, the effects of the Lenti-HKII shRNA therapy might be enhanced, and adverse effects related to high doses of ^{131}I can be avoided.

In the study, we obtained small-animal PET images of our mouse model with ^{18}F-FDG every week for up to 3 wk after tumor implantation to noninvasively assess responses to the therapies in the animal model (Fig. 6A). The Lenti-HKII shRNA therapy group showed a gradual increase of tumor ^{18}F-FDG uptake on days 14 and 21, compared with that observed on day 7. There was a possibility that low tumor ^{18}F-FDG uptake in mice treated with Lenti-HKII shRNA is related to HKII knockdown, which reduces ^{18}F-FDG phosphorylation rather than tumor cell death. Changes in tumor ^{18}F-FDG uptake were considerably smaller than changes in tumor volume as measured by calipers 14 d after starting the therapies.

jnm090266-pm ■ 10/12/11

RGB

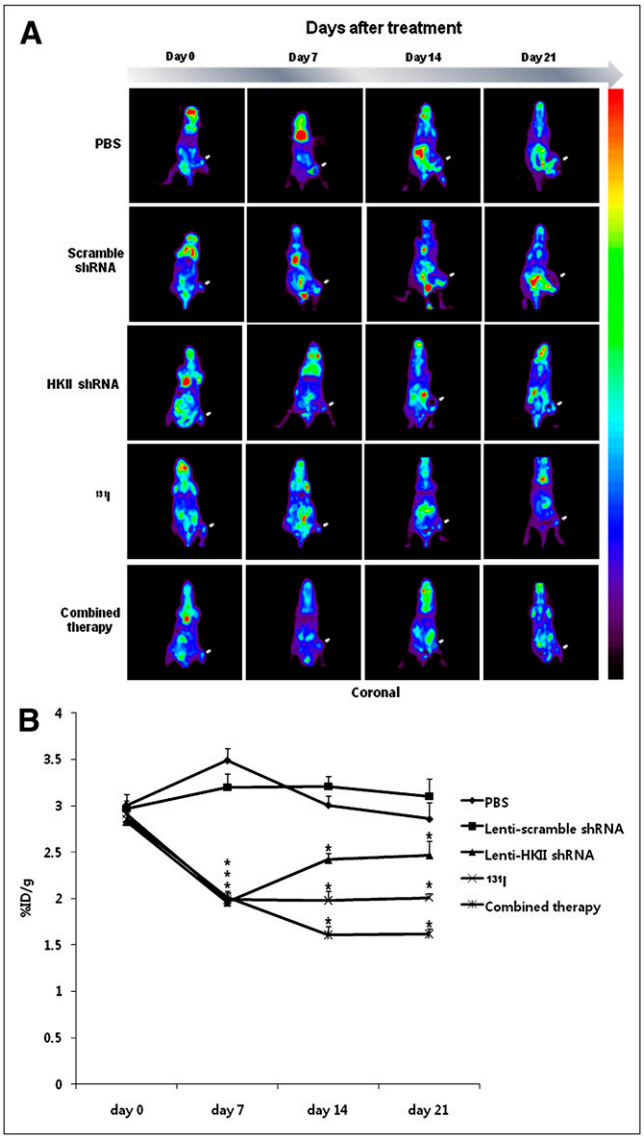

FIGURE 6. (A) ^{18}F-FDG small-animal PET was performed in vivo before and at 7, 14, and 21 d after Lenti-HKII shRNA, ^{131}I, or combined therapies. (B) Quantitated %ID/g data of ^{18}F-FDG uptake. ^{18}F-FDG uptake of ARO-NG tumor xenografts was inhibited by Lenti-HKII shRNA, ^{131}I therapy, and combined therapies. Lenti-HKII shRNA therapy group showed gradual increase of tumor ^{18}F-FDG uptake on days 14 and 21, compared with that of day 7. ^{131}I therapy group showed similar levels of tumor ^{18}F-FDG uptake on days 14 and 21, compared with day 7. Combined therapy group showed lowest tumor ^{18}F-FDG uptake on days 14 and 21, compared with other groups receiving individual therapies. *Mean $P < 0.05$. Arrows = location of ARO-NG tumors.

Despite the continuous tumor growth observed in the control and Lenti-scramble shRNA therapy groups, tumor ^{18}F-FDG uptake was decreased by days 14 and 21, compared with day 7. This decrease might have been related to central necrosis of the rapid-growing tumors in the control and Lenti-scramble shRNA therapy groups. However, results of the current study demonstrated that ^{18}F-FDG imaging can be used to measure the antitumor effects of ^{131}I, Lenti-HKII shRNA, and combined therapies. This approach may have limited clinical use because our study involved cell lines stably expressing the hNIS gene. An efficient therapeutic gene delivery method is a prerequisite for developing a successful in vivo hNIS gene therapy. To our best knowledge, the current study is the first to demonstrate the therapeutic effects of HKII shRNA delivered by lentivirus in a tumor-bearing animal model. Our results also showed that the combined use of HKII shRNA and ^{131}I treatment with hNIS gene therapy in ATC had the enhanced therapeutic effect both in vitro and in vivo.

CONCLUSION

The therapeutic effects of Lenti-HKII shRNA therapy or ^{131}I treatment with hNIS gene therapy alone on ATC were demonstrated in a mouse model. The combined ^{131}I and hNIS gene therapy with Lenti-HKII shRNA therapy resulted in a stronger antitumor effect than either the ^{131}I with hNIS gene therapy or HKII shRNA therapy alone. This combination therapy could be used as a powerful strategy for treating ATC, with relatively low radioiodine doses, compared with radioiodine hNIS gene therapy alone.

DISCLOSURE STATEMENT

The costs of publication of this article were defrayed in part by the payment of page charges. Therefore, and solely to indicate this fact, this article is hereby marked "advertisement" in accordance with 18 USC section 1734.

ACKNOWLEDGMENTS

This work was supported by the Nuclear Research and Development Program of the National Research Foundation of Korea (NRF) funded by the Ministry of Education, Science and Technology (MEST); a grant from the Korean MEST (the Regional Core Research Program/Anti-Aging and Well-Being Research Center); and the Brain Korea 21 Project in 2010. No other potential conflict of interest relevant to this article was reported.

REFERENCES

1. Are C, Shaha AR. Anaplastic thyroid carcinoma: biology, pathogenesis, prognostic factors, and treatment approaches. *Ann Surg Oncol.* 2006;13:453–464.
2. Haigh PI, Ituarte PH, Wu HS, et al. Completely resected anaplastic thyroid carcinoma combined with adjuvant chemotherapy and irradiation is associated with prolonged survival. *Cancer.* 2001;91:2335–2342.
3. Yau T, Lo CY, Epstein RJ, Lam AK, Wan KY, Lang BH. Treatment outcomes in anaplastic thyroid carcinoma: survival improvement in young patients with localized disease treated by combination of surgery and radiotherapy. *Ann Surg Oncol.* 2008;15:2500–2505.
4. Mathupala SP, Ko YH, Pedersen PL. Hexokinase-2 bound to mitochondria: cancer's stygian link to the "Warburg Effect" and a pivotal target for effective therapy. *Semin Cancer Biol.* 2009;19:17–24.
5. Pelicano H, Martin DS, Xu RH, Huang P. Glycolysis inhibition for anticancer treatment. *Oncogene.* 2006;25:4633–4646.
6. Warburg O. On the origin of cancer cells. *Science.* 1956;123:309–314.
7. Wilson JE. Isozymes of mammalian hexokinase: structure, subcellular localization and metabolic function. *J Exp Biol.* 2003;206:2049–2057.

8. Wilson JE. An introduction to the isoenzymes of mammalian hexokinase types I-III. *Biochem Soc Trans.* 1997;25:103–107.
9. Brummelkamp TR, Bernards R, Agami R. A system for stable expression of short interfering RNAs in mammalian cells. *Science.* 2002;296:550–553.
10. Esmaeili F, Bamdad T, Ghasemi S. Stable suppression of gene expression by short interfering RNAs targeted to promoter in a mouse embryonal carcinoma stem cell line. *In Vitro Cell Dev Biol Anim.* 2010;46:834–840.
11. Ahn KJ, Hwang HS, Park JH, et al. Evaluation of the role of hexokinase type II in cellular proliferation and apoptosis using human hepatocellular carcinoma cell lines. *J Nucl Med.* 2009;50:1525–1532.
12. Palmieri D, Fitzgerald D, Shreeve SM, et al. Analyses of resected human brain metastases of breast cancer reveal the association between up-regulation of hexokinase 2 and poor prognosis. *Mol Cancer Res.* 2009;7:1438–1445.
13. Bluff JE, Amarzguioui M, Slattery J, Reed MW, Brown NJ, Staton CA. Anti-tissue factor short hairpin RNA inhibits breast cancer growth in vivo. *Breast Cancer Res Treat.* 2011;128:691–701.
14. Sliva K, Schnierle BS. Selective gene silencing by viral delivery of short hairpin RNA. *Virol J.* 2010;7:248.
15. Barton GM, Medzhitov R. Retroviral delivery of small interfering RNA into primary cells. *Proc Natl Acad Sci USA.* 2002;99:14943–14945.
16. Rubinson DA, Dillon CP, Kwiatkowski AV, et al. A lentivirus-based system to functionally silence genes in primary mammalian cells, stem cells and transgenic mice by RNA interference. *Nat Genet.* 2003;33:401–406.
17. Chung JK. Sodium iodide symporter: its role in nuclear medicine. *J Nucl Med.* 2002;43:1188–1200.
18. Smit JW, Shroder-van der Elst JP, Karperien M, et al. Reestablishment of in vitro and in vivo iodide uptake by transfection of the human sodium iodide symporter (hNIS) in a hNIS defective human thyroid carcinoma cell line. *Thyroid.* 2000;10:939–943.
19. Lee YJ, Chung JK, Shin JH, et al. In vitro and in vivo properties of a human anaplastic thyroid carcinoma cell line transfected with the sodium iodide symporter gene. *Thyroid.* 2004;14:889–895.
20. Lee YL, Lee YJ, Ahn SJ, et al. Combined radionuclide-chemotherapy and in vivo imaging of hepatocellular carcinoma cells after transfection of a triple-gene construct, NIS, HSV1-sr39tk, and EGFP. *Cancer Lett.* 2010;290:129–138.
21. Hsieh YJ, Ke CC, Liu RS, et al. Radioiodide imaging and treatment of ARO cancer xenograft in a mouse model after expression of human sodium iodide symporter. *Anticancer Res.* 2007;27:2515–2522.
22. Vinuela E, Salas M, Sols A. Glucokinase and hexokinase in liver in relation to glycogen synthesis. *J Biol Chem.* 1963;238:1175–1177.
23. Jang JY, Choi Y, Jeon YK, Kim CW. Suppression of adenine nucleotide translocase-2 by vector-based siRNA in human breast cancer cells induces apoptosis and inhibits tumor growth in vitro and in vivo. *Breast Cancer Res.* 2008;10:R11.
24. Sledz CA, Williams BR. RNA interference and double-stranded-RNA-activated pathways. *Biochem Soc Trans.* 2004;32:952–956.
25. Peng Q, Zhou Q, Zhou J, Zhong D, Pan F, Liang H. Stable RNA interference of hexokinase II gene inhibits human colon cancer LoVo cell growth in vitro and in vivo. *Cancer Biol Ther.* 2008;7:1128–1135.
26. Maheshwari YK, Hill CS Jr, Haynie TP 3rd, Hickey RC, Samaan NA. ^{131}I therapy in differentiated thyroid carcinoma: M. D. Anderson Hospital experience. *Cancer.* 1981;47:664–671.
27. Smit JW, Schroder-van der Elst JP, Karperien M, et al. Iodide kinetics and experimental ^{131}I therapy in a xenotransplanted human sodium-iodide symporter-transfected human follicular thyroid carcinoma cell line. *J Clin Endocrinol Metab.* 2002;87:1247–1253.
28. Cengic N, Baker CH, Schutz M, Goke B, Morris JC, Spitzweg C. A novel therapeutic strategy for medullary thyroid cancer based on radioiodine therapy following tissue-specific sodium iodide symporter gene expression. *J Clin Endocrinol Metab.* 2005;90:4457–4464.
29. Hyer SL, Newbold K, Hamer CL. Early and late toxicity of radioiodine: detection and management. *Endocr Pract.* 2010;16:1064–1070.
30. Verhagen JN, Van der Heijden MC, Rijksen G, Der Kinderen PJ, Van Unnik JA, Staal GE. Determination and characterization of hexokinase in thyroid cancer and benign neoplasms. *Cancer.* 1985;55:1519–1524.
31. Peng QP, Zhou JM, Zhou Q, Pan F, Zhong DP, Liang HJ. Downregulation of the hexokinase II gene sensitizes human colon cancer cells to 5-fluorouracil. *Chemotherapy.* 2008;54:357–363.
32. Guo-Qing P, Yuan Y, Cai-Gao Z, Hongling Y, Gonghua H, Yan T. A study of association between expression of hOGG1, VDAC1, HK-2 and cervical carcinoma. *J Exp Clin Cancer Res.* 2010;29:129.

jnm090266-pm ■ 10/12/11